Progress In Electromagnetics Research C, Vol. 77, 185–193, 2017

Compact 3D Monopole Antenna for Different Wireless Communication Applications

Dalia M. Elsheakh* **and Esmat A. Abdel Fattah**

Abstract—A 3D compact printed monopole antenna for most of the wireless communication applications is proposed in this paper. The proposed antenna has dimensions $40 \times 30 \times 1.6\,\text{mm}^3$; it is based on multi different length arms of E-shaped monopole with modified ground plane coupled with meander line. The performance of the 3D antenna is almost the same as a 2D antenna with reduction in size, and it could be fit in a wireless transceiver device. The size reduction about 25% compared to the 2D planar proposed antenna is realized on a printed circuit board to reduce the fabrication cost. The coupling between the antenna elements broadens the operating bandwidth, which includes most of the wireless commercial service bands, GSM1800/GSM1900/ UMTS/WCDMA2100 802.11b/g/LTE2600 (2690 MHz) as well as 802.11a/n (5150–5825 MHz). The antenna's simulated and experimental results are in good agreement. It is fabricated on a low-cost FR4 substrate and measured to validate the simulation performances. Measured results display that the proposed antenna produces omnidirectional radiation pattern of −6 dB impedance bandwidth at multi operating bands and average gain of 3.5 dBi and 2 dBi for 2D and 3D, respectively over the operating band.

1. INTRODUCTION

Recently, increased use and reliance of commercial wireless communications in terms of technology, level of integration, and miniaturization are noticeable. There is a necessity for space/volume reduction and increase in antenna functionality. Wireless communication applications such as GSM/UMTS/LTE-WWAN/WLAN systems in laptops and other digital devices with wireless network access functions are very popular [1]. However, there is considerable challenge to realize a small internal multiband antenna design to fit in new portable systems. Extensive research activities have been published toward the development of multiband antennas for wireless USB dongle applications [2, 3], monopole antennas [4–6], and planar inverted-F antennas [6]. However, these complicated antennas cannot cover bandwidths broad enough for future communication requirements, especially for GSM 1800/1900/UMTS 2100 and LTE700/2300/2500 bands [12]. Printed antennas are very charming for a variety of commercial and military applications. However, they suffer from narrow bandwidth and large size as the frequency is lowered. Meander lines are introduced to increase the effective length of the current path with the aim to miniaturize the antenna which leads to the reduction of the antenna size.

In this paper, a compact multiband three-dimensional monopole antenna for wireless applications is proposed. Compact antennas are provided esthetics, safety, cost, aerodynamics, and physical size constraints due to system considerations. Low-profile antenna is used in a vehicle or handheld wireless devices to receive both a satellite positioning signal and cellular mobile. The proposed antenna consists of three arms with different lengths as an E-shaped monopole antenna, modified ground plane as a trapezoidal shaped with a meander-line [7], and each is responsible for certain bands of operation. The antenna satisfies −6 dB reflection coefficient which is sufficient for wireless broadband GSM

Received 6 July 2017, Accepted 23 August 2017, Scheduled 6 September 2017
* Corresponding author: Dalia Mohammed Nasha Elsheakh (daliaelsheakh@eri.sci.eg).
The authors are with the Electronics Research Institute, Cairo, Egypt.

1800 MHz, WiBro, 2.3–2.4 GHz, wireless local area network WLAN, 2.4–2.485 and 5.15–5.825 GHz), world interoperability for microwave access (WiMAX, 2.5–2.7 GHz), and most of LTE bands and satellite digital multimedia broadcasting (S-DMB, 2.605–2.655 GHz) services [13]. For portable wireless devices, the suitable antenna bandwidth is −6 dB as in [8–11]. All simulations are carried out using the EM commercial simulator high frequency structure simulator (HFSS) version 14.0, which is based on the finite-element numerical method. The design of the proposed antenna is introduced in the next section. The results and detail discussion about the proposed antenna are presented in Section 2. Then summaries of the proposed antenna designs for both 2D and 3D are presented in Section 4.

2. DESIGN OF PROPOSED ANTENNA

Three dimensions printing offers the chance to take the antenna off the PCB and integrate the antenna into the case or structure thus freeing the antenna designer from cramped circuit board areas while allowing increased antenna efficiency with larger designs. The design of the proposed antenna is started by evolution geometry of the proposed 2D antenna as shown in Fig. 1. Three steps of improving the developed antenna are shown in Fig. 2 from Antenna-1 to Antenna-3.

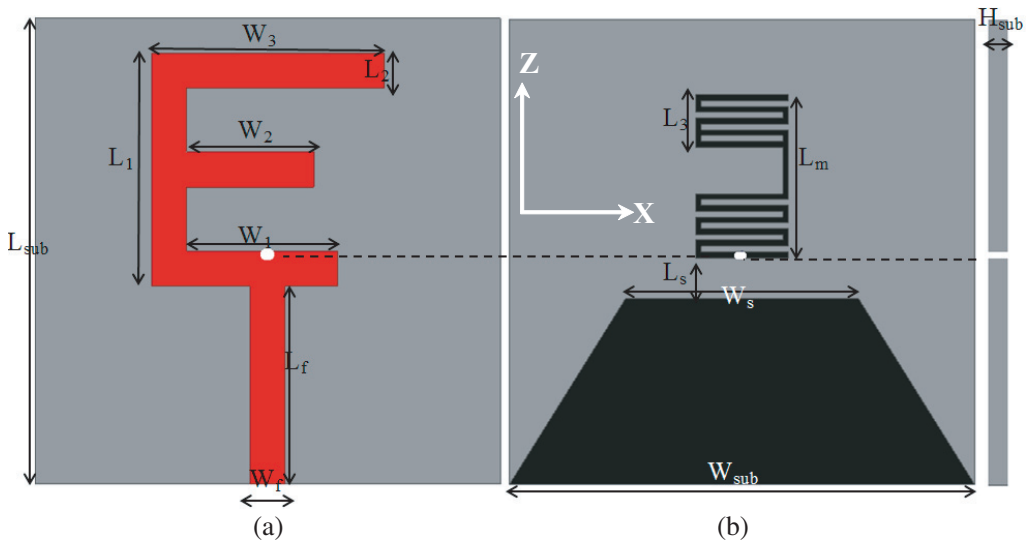

Figure 1. Layout of the proposed 2D antenna, (a) top layer, (b) bottom layer and (c) side view.

Firstly, a C-shaped monopole as shown in Fig. 2(a) with different arm lengths is used to create 1.9 GHz. Secondly, a straight strip is introduced, and the patch becomes the modified E-shape shown in Fig. 2(b). As a result, the lower frequency is slightly shifted to 1.85 GHz, and the impedance matching of the 2nd and 3rd resonant frequencies is improved as shown in Fig. 3(a).

Then, a trapezoidal ground plane as shown in Fig. 2(c) is used for the resonant mode of 6.5 GHz improvement. However, the impedance matching at 4–5.5 GHz is the worst. Finally, to remedy this effect, a meander line is added placed on the same side of ground plane. The E-shaped patch and meandered shape are electrically connected via a shorting pin as shown in Fig. 2(d). The meander line is used to create multiband operation at different frequencies and add their compactness as shown in Fig. 3(a). The performance after every design step is shown in Fig. 3(a).

All optimized dimensions are shown in Table 1. The proposed antenna occupies a volume about $40 \times 40 \times 1.6\,\text{mm}^3$. To fit a package, the antenna is folded in 3D, and its reflection coefficient is improved due to coupling between the antenna elements as shown in Fig. 2(e), hence the antenna volume is now $3\times\ (40 \times 10 \times 1.6)\,\text{mm}^3$, i.e., the reduction in the antenna volume is about 25% from the original antenna size. The folded antenna is mounted on a commercial FR4 substrate with thickness of 1.6 mm and relative permittivity (ε_r) of 4.7. The folded antenna has almost the same behavior as the unfolded-one, as shown in Fig. 3(b). The conformality of the proposed antenna affects the antenna reflection

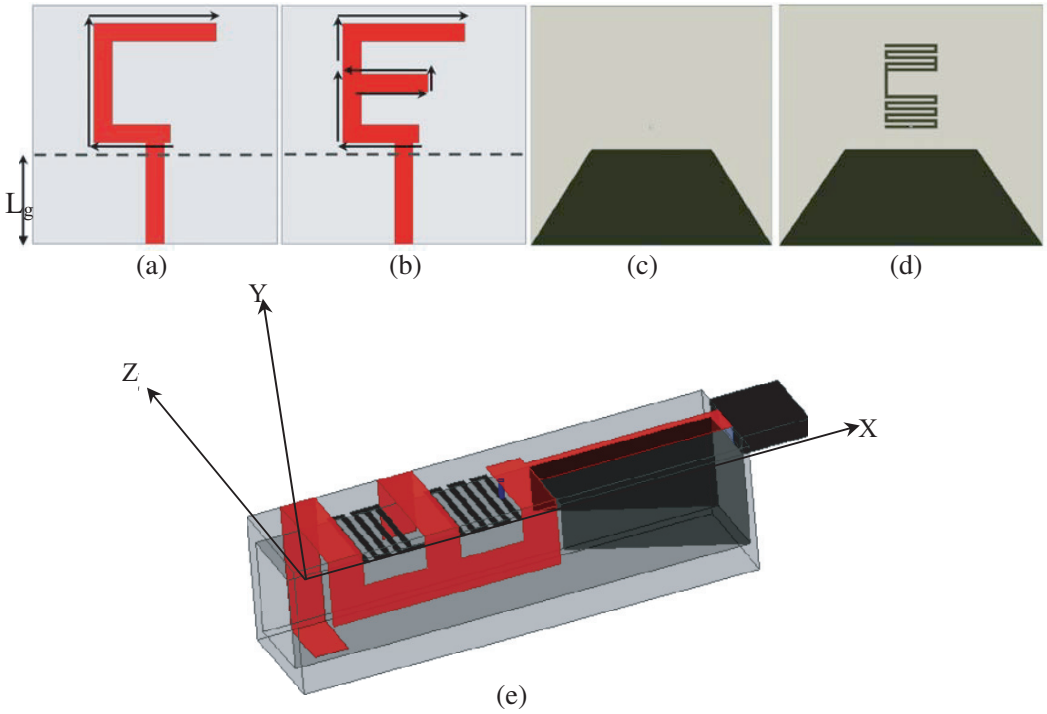

Figure 2. (a) Step one, (b) step two upper layer, (c) step three lower substrate layer and (d) step four and (e) 3D monopole.

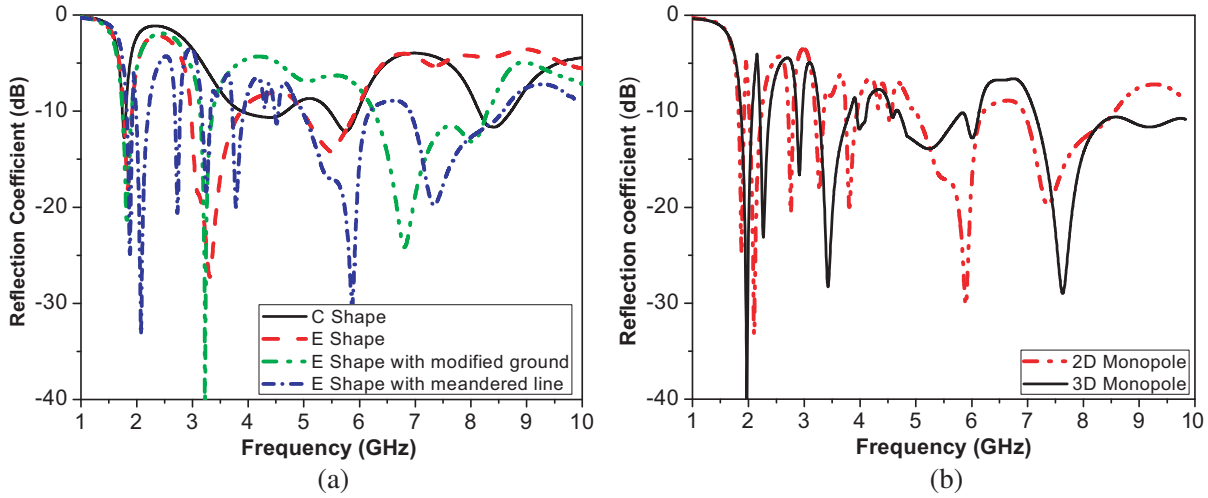

Figure 3. (a) Reflection coefficient of the design procedures of the proposed antenna and (b) $|S_{11}|$ of 2D and 3D.

coefficient slightly as shown in Fig. 3(b). Then the ground plane length is optimized to obtain good impedance matching from size 14 mm to 18 mm with step 2 mm, and the reflection coefficient results are shown in Fig. 4(a). The results show the optimum and wide bandwidth of operation at length 16 mm as shown in Fig. 4(a). On the other hand, the meander line dimensions are also optimized to improve the antenna multibands at desired operational bands. The dimension area of the meander line starts from $4 \times 0.25\,\text{mm}^2$ to be $10 \times 0.65\,\text{mm}^2$ on two dimensions steps as shown in Fig. 4(b). This figure shows that when small strip meander line area is used there are multiple frequencies created but not at desired bands of wireless communication applications.

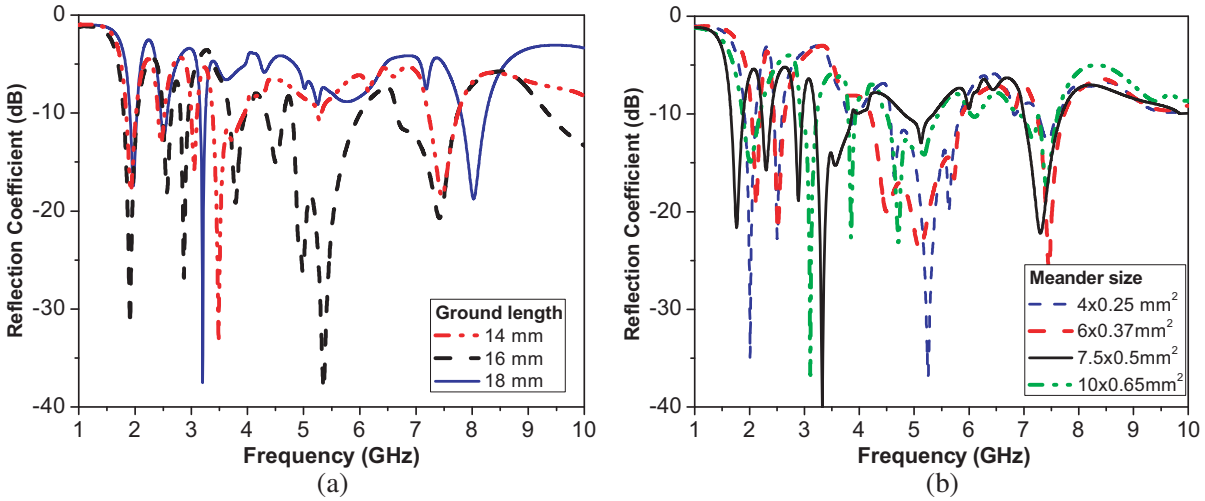

Figure 4. (a) Simulated S-parameters of proposed antenna with different ground plane length and (b) optimized of meander line dimensions.

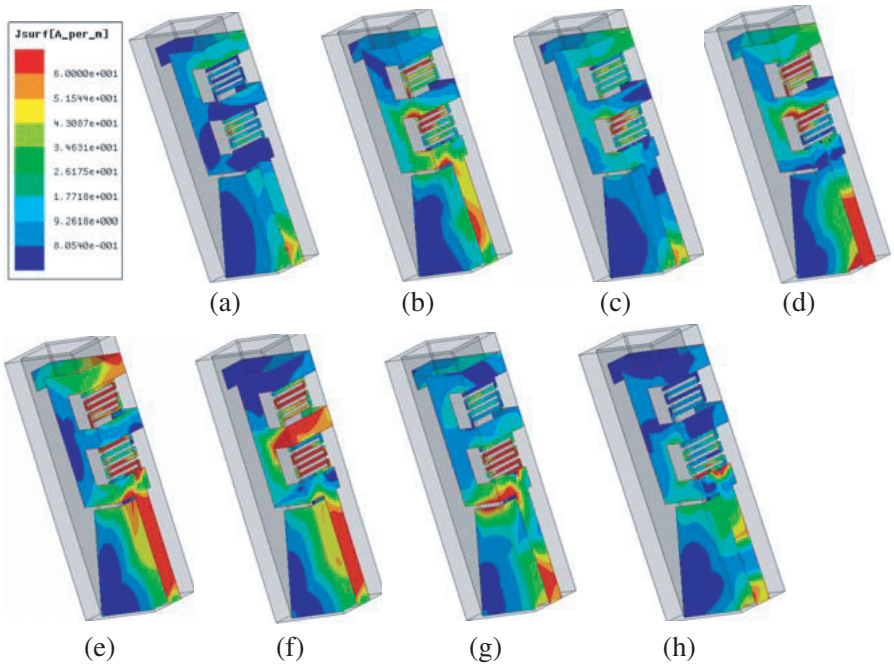

Figure 5. (a)–(h) Surface current densities for the proposed antenna at 1.8, 2.1, 2.4, 3.1, 3.5, 5.2, 5.8 and 6.8 GHz, respectively.

In order to evaluate the characteristics of the 3D monopole antenna in more details, the simulated surface current distributions on the printed metal portion at different frequencies are demonstrated in Figs. 5(a)–(h), respectively. Three dimensional (3D) plots are used to clarify the radiating element at each frequency. Red color represents the corresponding radiating element. The radiation tends to be broadside similar to those obtained for conventional internal patch antennas for mobile phone applications, and it follows the current distribution shown in Fig. 5. Moreover, the current on the via connected to the E-shaped monopole and meander line is small, and hence, it does not seriously affect the radiation.

3. RESULTS AND DISCUSSIONS

A prototype of the proposed antenna is fabricated by using photolithographic techniques on a commercial FR-4 substrate. The measurements are carried out by using a Rohde & Schwarz ZVA67 vector network analyzer operating from 50 MHz to 67 GHz. The antenna is fed by a 50 Ω coaxial cable as shown in Fig. 6. The 3D antenna is also fabricated by the same method as fabricating three rectangular substrate sides with width 10 mm and then assembled together by soldiering. The antenna characteristics such as reflection coefficient $|S_{11}|$, efficiency, and gain are shown in the following figures. The performances of antenna parameters for both proposed 2D and 3D antennas are measured as shown in the following section.

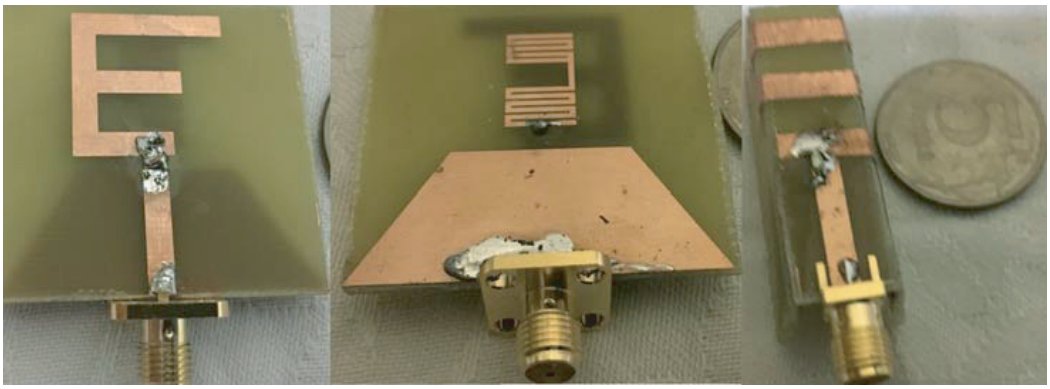

(a) (b) (c)

Figure 6. Fabricated proposed antenna, (a) upper side, (b) ground plane, and (c) 3D proposed antenna.

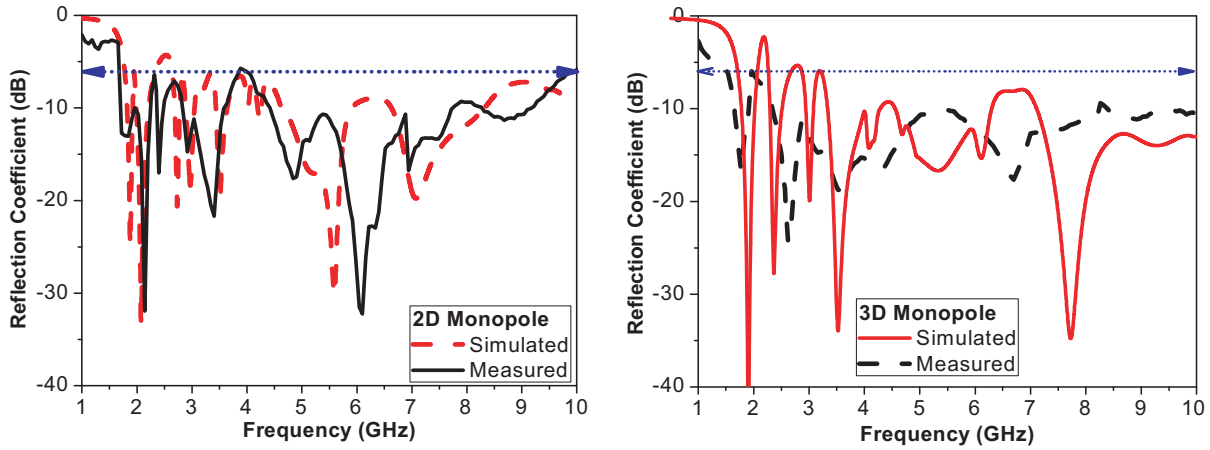

(a) (b)

Figure 7. Comparison of $|S_{11}|$ between simulated and measured results, (a) 2D and (b) 3D proposed antenna.

Table 1. Dimensions of the proposed antenna (all dimensions in mm).

L_{sub}	W_{sub}	L_f	W_f	L_1	L_2	W_s
40	*40*	*18*	*3*	*20*	*3*	*20*
W_1	W_2	W_3	L_m	L_3	L_s	H_{sub}
17	*14*	*20*	*13*	*3*	*1*	*1.6*

Table 2. Radiation efficiency and gain for both proposed two and three dimensions antennas.

Frequency (GHz)	Radiation efficiency (%)		Antenna gain (dBi)	
	2D	3D	2D	3D
GSM (1.8, 1.83, 1.88)	59, 60, 62	42, 51, 55	3.5, 4, 4.2	1.2, 1.5, 1.8
UTMS (1.9, 2, 2.1)	68, 69, 73	75, 75, 89	4.8, 5, 2.5	1.5, 1.2, 1.1
ISM (2.4–2.5)	60	55	4	2
$W_{\max}$ (3.5, 3.8)	69, 64	70, 84	−1, −3	0.3, 1
WLAN (5.2, 5.8)	70, 65	80, 84	−0.5, −1	1.1, 1.3

Table 3. Simulated radiation patterns of the proposed 3D monopole in $\Phi = 0°$ —, $\Phi = 90°$ - - - and $= 90°$ - ·· - at the different frequencies.

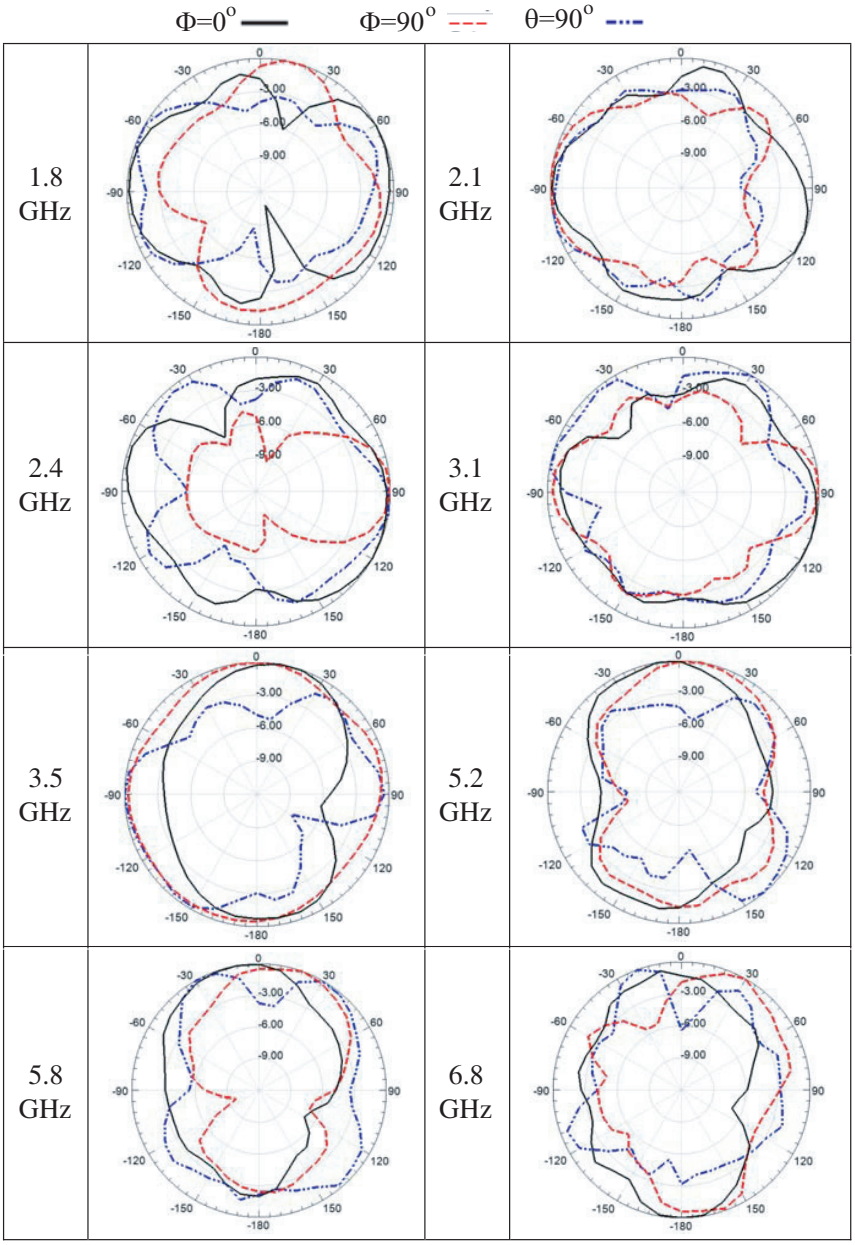

Table 4. Comparison between measured and simulated radiation patterns of 3D monopole antennas in both XY and YZ planes at different frequencies 1.8 GHz, 2.4 GHz, 5.2 GHz and 6.8 GHz.

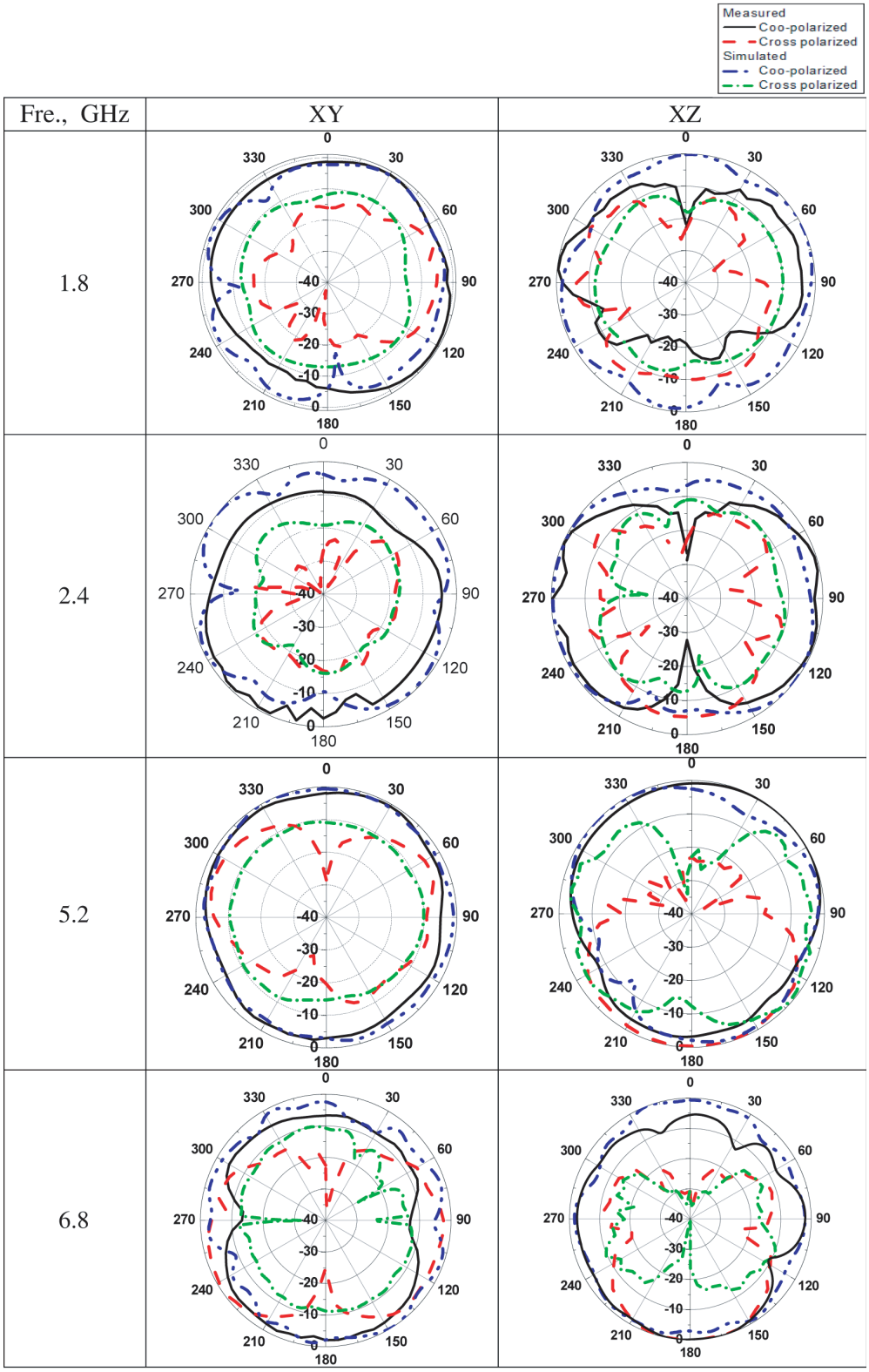

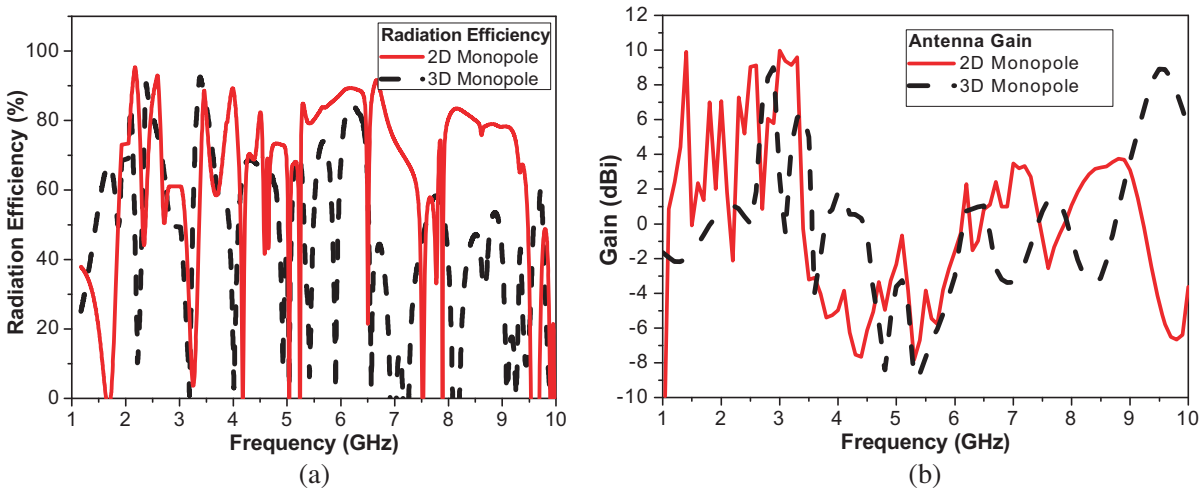

Figure 8. (a)–(b) Simulated monopole antenna radiation efficiency and gain for both 2D and 3D antenna, respectively.

The simulated and measured input reflection coefficients $|S_{11}|$ of the antennas are shown in Figs. 7(a) and (b) for 2D and 3D antennas, respectively. The results are found in very good agreement, as shown in Fig. 7. The −6 dB impedance bandwidth of the proposed monopole antenna is extended from 1.7 GHz to 1 GHz to cover most wireless applications. Then the measured results of the radiation efficiency by using wheeler cap method [15–17] is done by using a horn antenna to completely covering the proposed antennas as shown in Fig. 8(a). The average radiation efficiency is around 70%, 62% over the operating bands for 2D and 3D antennas, respectively as shown in Fig. 8(a).

The 2D and 3D monopole antennas achieve simulated average gain of 3.5 dBi, 2 dBi and the peak realized gain around 8.5 dBi at 2.7 GHz and 2.95 GHz respectively as shown in Fig. 8(b). The antenna radiation efficiency is simulated for the proposed 2D and 3D antennas. Table 2 shows the value of the radiation efficiency and antenna gain at certain wireless communication applications.

Table 3 shows the simulated 2D radiation patterns in three principal planes, namely, ($\varphi = 0$), ($\varphi = 90$) and ($\theta = 90$) planes of the proposed 3D monopole antenna, at the selected operating frequencies including 1.8 GHz, 2.1 GHz, 2.4 GHz, 3.1 GHz, 3.5 GHz, 5.2 GHz, 5.8 GHz and 6.8 GHz. We observe dipole-like radiation patterns in the lower band and an omnidirectional radiation in the plane ($\varphi = 0$). The radiation patterns in the higher band in planes ($\varphi = 90$ and $\theta = 90$) display more variations and nulls. These characteristics are similar to those observed for the conventional internal monopole antenna. At 1 GHz, the radiation pattern corresponds to a monopole antenna in the XZ and XY planes, from 1.5 to 2.5 GHz which corresponds to a monopole in both planes. On the other hand, at 3.5 GHz, the radiation corresponds to a meander monopole in the XZ plane (each element). The antenna has radiation pattern of sufficiently low cross polarization in E-plane and H-plane, as depicted in the Table 4. The radiation pattern < -7.5 dBi in E-plane ($\Phi = 0$)(XY) and < -10 dBi in H-plane ($\theta = 90$) (XZ), where the antenna coordinate is shown in Figure 2. The measured results show good agreement with simulated ones, and there is about ±3 dBi difference on average over the operating band.

4. CONCLUSION

In this paper, a 3D monopole antenna is designed to fit in wireless communication devices that operate at many wireless communication bands applications as GSM (1.8 GHz), UMTS (1.9 to 2.1 GHz), WCDMA, Bluetooth, ISM, 802.11b/g (2.4 to 2.45 GHz), LTE (2.6 GHz), as well as 802.11a/n. The proposed antenna has an E-shaped monopole with a meander structure and modified ground plane. The proposed antenna is small enough to fit in handheld wireless devices. The antenna is successfully designed and implemented, and measured operational bandwidth is extended from 1.7 GHz to 10 GHz with average

radiation efficiency about 70% over the operating bands. The gain varies with frequency with average 3.5 and 2 dBi for 2D and 3D antennas, respectively. The antenna's radiation is nearly omnidirectional at different resonant frequencies. The proposed antenna is a good candidate for USB dongle applications.

ACKNOWLEDGMENT

Ain Shams University, Faculty of Engineering for measuring the radiation pattern of the proposed antennas.

REFERENCES

1. Lee, S. W., H. S. Jung, and Y. J. Sung, "A reconfigurable antenna for LTE/WWAN mobile handset applications," *IEEE Antennas and Wireless Propagation Letters*, Vol. 14, 48–51, 2016.
2. Park, Y. K, D. Kang, and Y. Sung, "Compact folded triband monopole antenna for USB dongle applications," *IEEE Antennas and Wireless Propagation Letters*, Vol. 11, 228–231, 2012.
3. Bakariya, P. S., S. Dwari, M. Sarkar, and M. K. Mandal, "Proximity coupled multiband microstrip antenna for wireless applications," *IEEE Antennas and Wireless Propagation Letters*, Vol. 14, 646–649, 2016.
4. Alsath, M. G. N., L. Lawrance, M. Kanagasbai, D. B. Rajendran, B. Moorthy, and J. V. George, "Quad-band diversity antenna for automotive environment," *IEEE Antennas and Wireless Propagation Letters*, Vol. 14, 875–878, 2016.
5. Tien, M. and M. L. Chuang, "Multi-broadband slotted bow-tie monopole antenna," *IEEE Antennas and Wireless Propagation Letters*, Vol. 14, 887–890, 2016.
6. Pazin, L. and L. Yehuda, "Inverted-F laptop antenna with enhanced bandwidth for Wi-Fi/WiMAX applications," *IEEE Trans. Antennas Propag.*, Vol. 59, No. 3, 1065–1068, 2011.
7. Yong, L. B., H. C. Jin, L. Ying, J. Joshua, L. W. Li, and W. Y. Jiang, "Ultra-wideband antenna for LTE/GSM/UMTS wireless USB dongle applications," *IEEE Antennas and Wireless Propagation Letters*, Vol. 11, 403–406, 2012.
8. Wong, K. L., Y. W. Chang, and S.-C. Chen, "Bandwidth enhancement of small-size planar tablet computer antenna using a parallel-resonant spiral slit," *IEEE Trans. Antennas Propag.*, Vol. 60, 1705–1711, 2012.
9. Zheng, M., H. Wang, and Y. Hao, "Internal hexa-band folded monopole/dipole/loop antenna with four resonances for mobile device," *IEEE Trans. Antennas Propag.*, Vol. 60, 2880–2885, June 2012.
10. Chang, S. H. and W.-J. Liao, "A broadband LTE/WWAN antenna design for tablet PC," *IEEE Trans. Antennas Propag.*, Vol. 60, No. 9, 4354–4359, 2012.
11. Li, Y., Z. Zhang, J. Zheng, Z. Feng, and M. Iskander, "A compact heptaband loop-inverted F reconfigurable antenna for mobile phone," *IEEE Trans. Antennas Propag.*, Vol. 60, 389–392, 2012.
12. Lee, C. M. and C. W. Jung, "Radiation pattern reconfigurable antenna using monopole loop for fibit flex wristband," *IEEE Antennas and Wireless Propagation Letters*, Vol. 14, 269–272, 2016.
13. Yang, C. W., Y. B. Jung, and C. W. Jung, "Octaband internal antenna for 4G mobile handset," *IEEE Antennas and Wireless Propagation Letters*, Vol. 10, 817–819, 2011.
14. Lu, J. H. and F. C. Tsai, "Planar internal LTE/WWAN monopole antenna for tablet computer application," *IEEE Trans. Antennas Propag. Letter*, Vol. 10, No. 8, 4358–4363, 2011.
15. Johnston, R. H. and J. G. Mc Rory, "An improved small antenna radiation efficiency measurement method," *IEEE AP-Magazine*, Vol. 40, 40–48, 1998.
16. Raiva, A. P. and J. F.Sanchez, "A rectangular cavity for cell phone antenna efficiency measurement," *IEEE Antenna Propagation, Symp.*, Washington, DC, USA, July 3–8, 2005.
17. Pozar, D. M. and B. Kaufman, "Comparison of three methods for the measurement of printed antenna efficiency," *IEEE Trans. Antennas Propag.*, Vol. 36, 136–139, January 1988.